Biosensors and Bioelectronics 139 (2019) 111326

Contents lists available at ScienceDirect

Biosensors and Bioelectronics

journal homepage: www.elsevier.com/locate/bios

EGFR point mutation detection of single circulating tumor cells for lung cancer using a micro-well array

Wanlei Gao[a,b], Xiaofen Zhang[c], Haojun Yuan[b], Yanmin Wang[b], Hongbo Zhou[b], Han Jin[a], Chunping Jia[b,*], Qinghui Jin[a,**], Hui Cong[c,***], Jianlong Zhao[a]

[a] The Faculty of Electrical Engineering and Computer Science, Ningbo University, Ningbo, Zhejiang, 315211, China
[b] State Key Laboratories of Transducer Technology, Shanghai Institute of Microsystem and Information Technology, Chinese Academy of Sciences, Shanghai, 200050, China
[c] Center of Laboratory Medicine, Affiliated Hospital of Nantong University, Nantong, Jiangsu, 226000, China

ARTICLE INFO

Keywords:
Circulating tumor cells (CTCs)
Micro-well array
Lung cancer
EGFR point mutation
Single-cell genetic analysis
Heterogeneity

ABSTRACT

In view of their critical function in metastasis, characterization of single circulating tumor cells (CTCs) can provide important clinical information to monitor tumor progression and guide personal therapy. Single-cell genetic analysis methods based on microfluidics have some inherent shortcomings such as complicated operation, low throughput, and expensive equipment requirements. To overcome these barriers, we developed a simple and open micro-well array containing 26,208 units for either nuclear acids or single-cell genetic analysis. Through modification of the polydimethylsiloxane surface and optimization of chip packaging, we addressed protein adsorption and solution evaporation for PCR amplification on a chip. In the detection of epidermal growth factor receptor (EGFR) exon gene 21, this micro-well array demonstrated good linear correlation at a DNA concentration from 1×10^1 to 1×10^5 copies/μL ($R^2 = 0.9877$). We then successfully integrated cell capture, lysis, PCR amplification, and signal read-out on the micro-well array, enabling the rapid and simple genetic analysis of single cells. This device was used to detect duplex EGFR mutation genes of lung cancer cell lines (H1975 and A549 cells) and normal leukocytes, demonstrating the ability to perform high-throughput, massively parallel duplex gene analysis at the single-cell level. Different types of point mutations (EGFR-L858R mutation or EGFR-T790M mutation) were detected in single H1975 cells, further validating the significance of single-cell level gene detection. In addition, this method showed a good performance in the heterogeneity detection of individual CTCs from lung cancer patients, required for micro-invasive cancer monitoring and treatment selection.

1. Introduction

Due to its low sensitivity of early diagnosis and high rates of relapse (Katanoda et al., 2018; O'Flaherty et al., 2012), lung cancer is the leading cause of cancer-related deaths worldwide. In recent years, new molecular targeted therapies have had a significant effect on the prolongation of survival in lung cancer patients with specific gene mutations such as epidermal growth factor receptor (EGFR) and anaplastic lymphoma kinase(Lin et al., 2016; Lu et al., 2018; Rothschild, 2016). However, certain mutations (such as T790M) lead to the loss of drug binding and subsequent drug resistance in non-small-cell lung carcinoma patients (Maheswaran et al., 2008; Wu et al., 2012; Zou et al., 2017). Gene mutations are commonly detected through gene sequencing of cells from lesion tissue (Alberter et al., 2016; Dancey et al., 2012). However, tissue biopsy is highly invasive and not suitable in the evaluation of efficacy of lung cancer treatment or in monitoring the dynamic changes of tumor cell genotypes.

Given the limitations of tissue biopsy, the liquid biopsy technique has been developed in recent years as a simple, rapid, and minimally invasive detection method. Excessively expressed proteins, nucleic acids, and rare tumor cells in blood are closely related to the development of cancer. Circulating tumor cells (CTCs) from cancerous organs are transferred to other organs through the circulatory system to form new cancerous sites(Krebs et al., 2014). Therefore, CTC mutational

* Corresponding author. Shanghai Institute of Microsystem and Information Technology, Chinese Academy of Science, 865 Changning Road, Shanghai, 200050, China.
** Corresponding author. The Faculty of Electrical Engineering and Computer Science, Ningbo University, Ningbo, Zhejiang, 315211, China.
*** Corresponding author. Center of Laboratory Medicine, Affiliated Hospital of Nantong University, 20 Xisi Road, Nantong, Jiangsu, 226000, China.
E-mail addresses: jiachp@mail.sim.ac.cn (C. Jia), jinqinghui@nbu.edu.cn (Q. Jin), huicjs@163.com (H. Cong).

https://doi.org/10.1016/j.bios.2019.111326
Received 14 February 2019; Received in revised form 26 April 2019; Accepted 13 May 2019
Available online 14 May 2019
0956-5663/

gene types may represent the genetic information of local and metastatic tumor cells. More importantly, CTCs can be obtained through routine blood collection and are suitable for providing guidance for the dynamic monitoring of cancer progression (Sundaresan et al., 2016; Tartarone et al., 2017).

However, most CTC detection platforms currently rely on immunehistochemical CTC count to characterize the development of tumors, which obviously cannot provide insight into the potential genetic information of CTCs(Myung and Hong, 2015; Tang et al., 2016). Previous studies have detected specific gene mutations by directly analyzing gene expression in bulk cells, yet these measurements are often contaminated by circulating tumor DNA, leukocytes, and other blood components (Devriese et al., 2012). Additionally, these detection methods average the differences in single CTCs and hardly recognize rare mutant genes presenting in individual CTCs. Indeed, the heterogeneity of CTCs is an important aspect in studying tumor progression and metastasis(Haber and Velculescu, 2014). Some multigene detection systems at the single-cell level have been developed for breast cancer and metastatic prostate cancer. Lin et al., (2014) designed a PN-Nanovelcro chip for CTC detection. Following trapping in the chip, single CTCs were recovered through laser cutting technology and detected by sequencing. Zhang et al.(Chen et al., 2013; Zhang et al., 2015) developed a microfluidic chip to detect single-cell genetic mutations of rare tumor cells. CTCs were trapped in nano-wells and retrieved using a micropipette for off-chip genome amplification and sequencing. Nevertheless, these methods are based on the manual selection of cells and therefore cannot realize high throughput detection, thus hindering their large-scale clinical application.

In recent years due to their advantages of having a functional unit size similar to that of cellular dimensions, their high precision, and fast detection, microfluidic systems have obvious advantages in rare cell detection (Shen et al., 2014; Yu et al., 2013). Valve-driven microfluidic systems(White et al., 2013), emulsion drop PCR systems(Novak et al., 2011), and micro-well detection systems(Haider et al., 2016) have been developed for single-cell gene detection. Gong et al., (2010) developed a micro-well chip for single-cell mRNA detection, relying on gravity to force single cells to settle in the micro-wells randomly. Nevertheless, this method is not suitable for detecting rare CTCs due to its high cell loss. White et al., (2013) developed a valve-controlled single-cell nucleic acid detection device that integrated single-cell trapping, lysing, reverse transcription, and digital PCR amplification. However, the device contained multiple valves to control the opening and closing of each chamber, and therefore its complicated operation and high-cost equipment represent obstacles for clinical application.

Given the above limitations, we developed a micro-well array-based method to detect gene mutation in single CTCs. The developed microfluidic chip contains more than 20,000 units for massive parallel duplex gene detection in a single cell, achieving a high loading rate of cells through centrifugation without the need for external pumping. Through the modification of PDMS and optimizing chip sealing, we achieved the integration of single-cell lysis, nucleic acid amplification, and gene mutation analysis on this simple chip. The detection platform proposed herein was then used to detect duplex gene mutation at the single-cell level for lung cancer cells and its clinical application in CTCs from lung cancer patients was verified, demonstrating its promising utility for genetic analysis of single CTCs.

2. Materials and methods

Experimental details and protocols for chip fabrication, micro-well array modification, cell culture and spiking, single cell loading, lysis, on-chip RT-PCR, signal readout and data analysis are provided in *Supplementary Information*.

3. Results and discussion

3.1. Cell loading and attachment during detection

To achieve high-throughput single-cell detection, we ensured the existence of a sufficiently high number of micro-wells for target cells. The cell distribution in the micro-wells was defined as a Poisson random variable X, given that the number of micro-wells (m) is much larger than that of cells (n) (Dimov et al., 2014). For a certain number of micro-wells, the probability of containing at most one cell for the micro-wells can be expressed as follows:

$$X \sim Pois\left(\frac{n}{m}\right)$$

$$P(X = k) = \frac{1}{k!}\left(\frac{n}{m}\right)^{k} exp\left(-\frac{n}{m}\right)$$

$$P(X \leq 1) = P(X = 0) + P(X = 1) = \left(1 + \frac{n}{m}\right) exp\left(-\frac{n}{m}\right)$$

In our analysis, each micro-well array contained 26,208 wells and detected approximately 2000 target cells (CTCs) from 2 mL of blood samples. According to the above formula, the probability of a micro-well containing either one cell or no cell was 99.7%. Therefore, the proposed micro-well array method can analyze single cells (approximately 2000 cells) at a high-throughput level.

The overall workflow of the proposed detection system is shown in Fig. 1. The whole process of detection involves the addition of a cell suspension on top of the chip; sealing of the chip with an adhesive film; heat lysis; removal of the adhesive film; addition of the PCR mix; re-sealing of the chip with glass and polypropylene film; RT-PCR on chip and read-out of fluorescence. In order to detect patient samples, the processed blood was incubated with anti-CD45 antibody-modified magnetic beads to enrich CTCs (Fig. 1A). The enriched cells were then processed with the micro-well array (Fig. 1B), loaded randomly in the micro-well array through centrifugation (Fig. S2). Therefore, the speed of centrifugation is the key factor to the rate of cell loading. The loading rate of cells, namely the ratio of the number of loaded cells to that of the number of cells added, varied with centrifugation speed (Fig. 2A).Three lung cancer cell lines(H446, A549, and H1975) were stained with DAPI and loaded in the micro-well array using different centrifugation speed, respectively. Between 100 and 300 rpm, the loading rate was below 90%, with the cells concentrating at the center of the chip. The chip reached a maximum recovery rate of 94% for H446 at 500 rpm (91% for A549, 90% for H1975). While at 700 rpm, some cells were forced into the gasket wall, resulting in a decrease in the number of loading cells. Therefore, a centrifugation speed of 500 rpm was used for subsequent cell loading. To verify the trapping of single cells in each micro-well, we tested the fraction of wells containing zero, single, or multiple cells for the loading of 2000 cells. The results showed that approximately 0.4% of all wells had two or more cells (Fig. S3). Therefore, to ensure single-cell analysis, an operational range of 0 and 2000 cells was used to fill less than 6% of wells with single cells and exclude multiple cells per well trapping.

For subsequent experiments, cells trapped in the micro-wells were required to stay in place during chip sealing and sampling. To assess this, H446 cells (approximately 100–2000) were added into the micro-wells and counted before and after chip sealing. The cells remained attached in the same micro-well and counts did not change after sealing. Therefore, chip sealing by PCR film did not affect cell placement. Finally, cells were imaged and analyzed in the micro-well array. Regression analysis showed that the slope for the line was 0.9301 ± 0.0095 ($R^2 = 0.9995$) (Fig. 2B), consistent with the maximum recovery rate (94%) in the centrifugation speed optimization of H446 cells. Thus, we speculated that most cell loss resulted from centrifugation for cell loading, while the follow-up processes of sealing

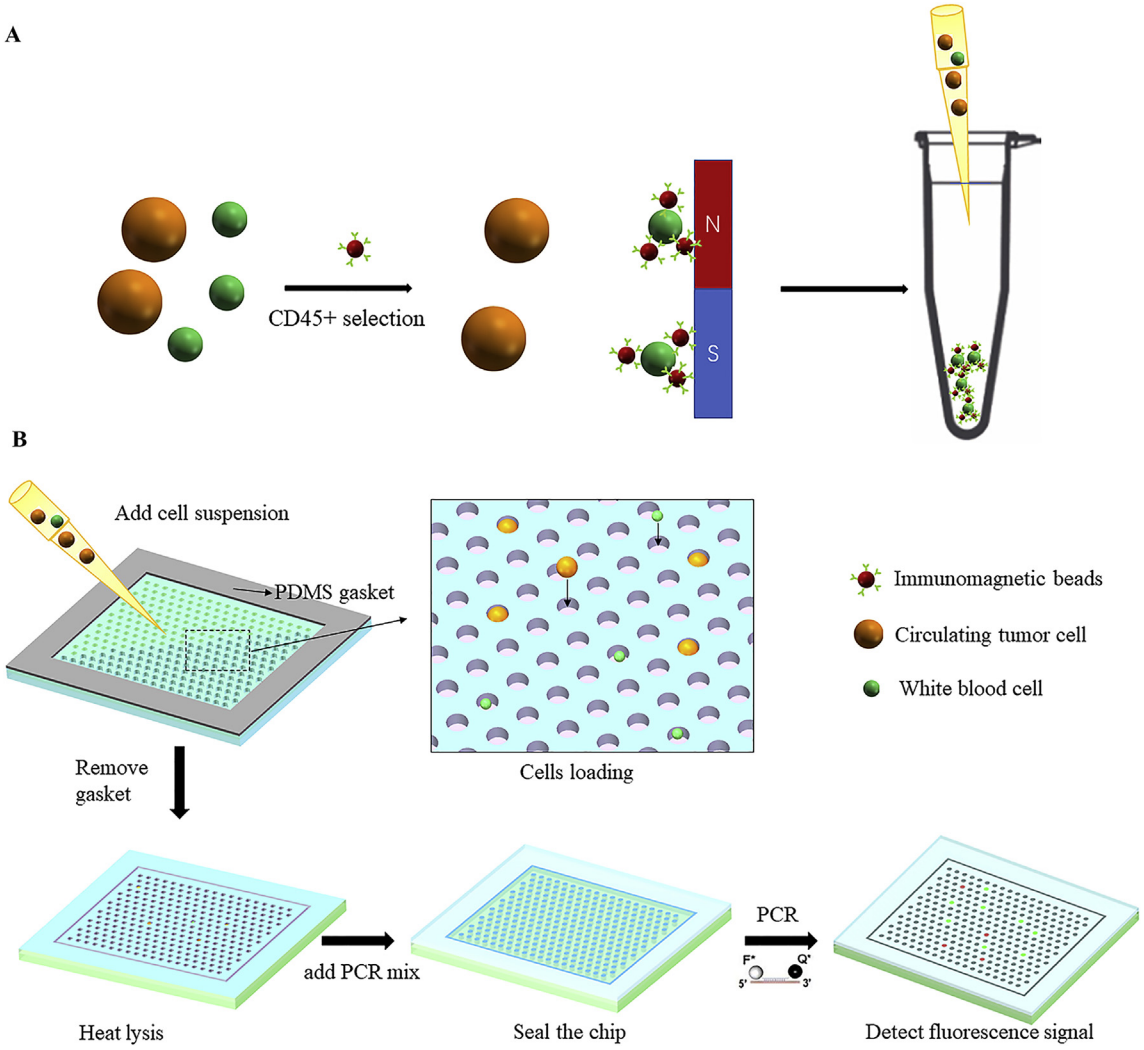

Fig. 1. Overall workflow of the integrated single-cell detection system. (A) Blood samples were processed fordepletion of white blood cells by CD45 magnetic beads; the supernatants are mostly all circulating-tumor cells. (B) All eluents were directly loaded onto the micro-well array device, and cells were seeded into individual compartments by centrifugation. After heating, the PCR mix was applied to the micro-wells, which were then sealed with PCR film and glass. The device was then placed into a thermocycler for PCR amplification. Multigene expression using up to two off-the-shelf hydrolysis probes with whole chip signals were imaged by fluorescence microscopy.

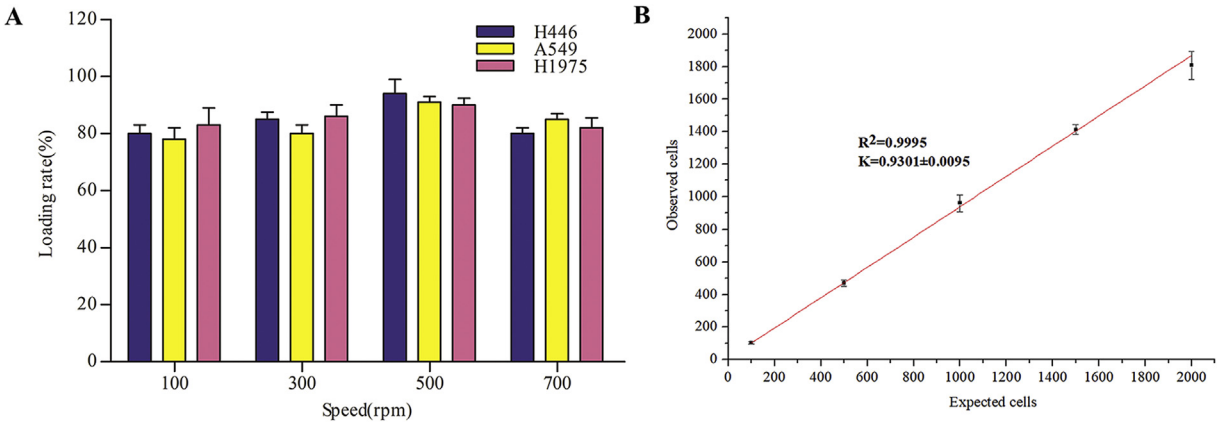

Fig. 2. Various conditions for cancer cell loading on micro-well array. (A) The effect of spin speed on the loading rate of H446, A549 and H1975 cells (using 1000 cells). (B) Capture efficiency of H446 cells from 100 to 2000 cells.

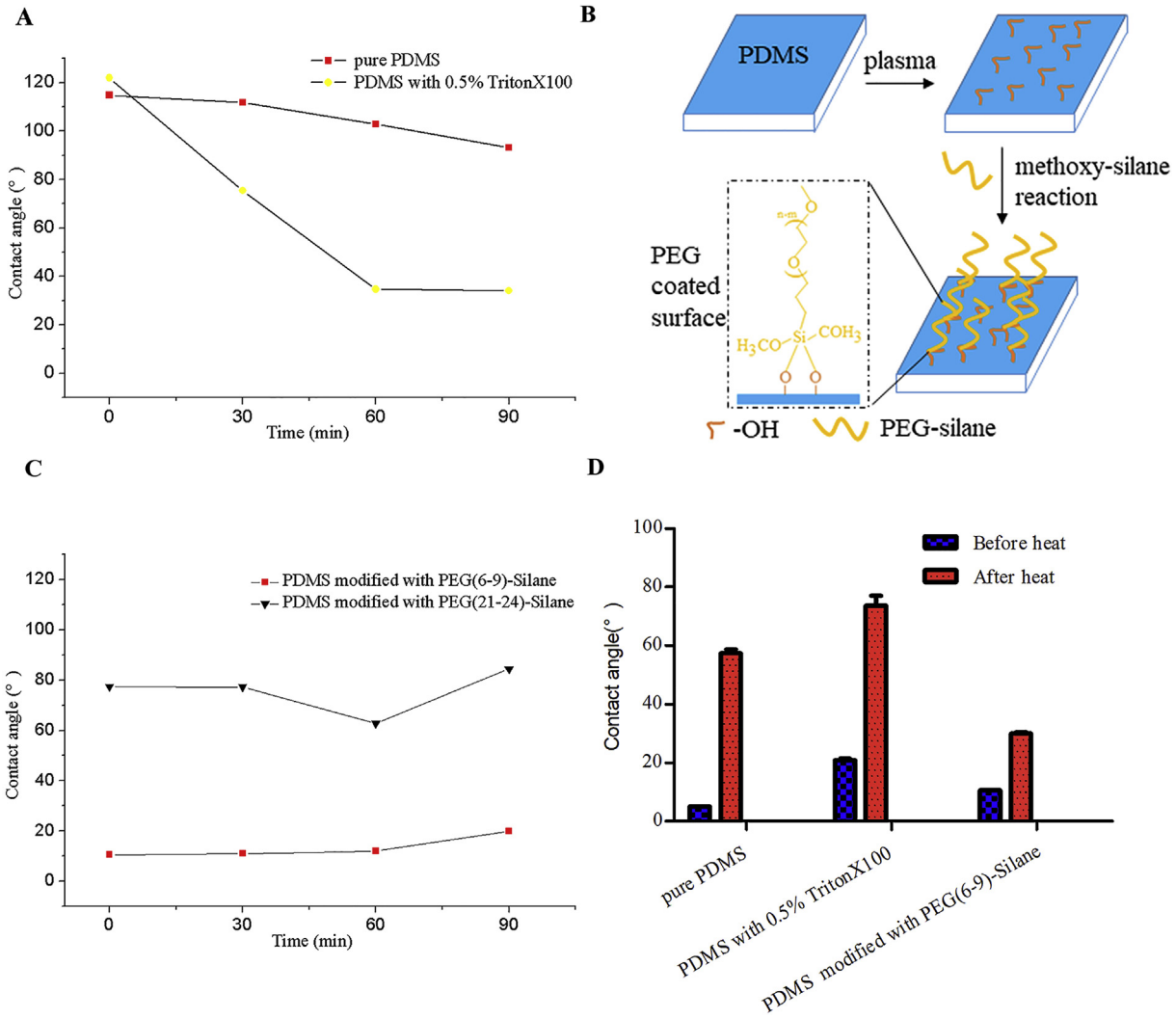

Fig. 3. Comparison of different modified methods for PDMS. (A) Dynamic change of water contact angle on pure PDMS and 0.5% TritonX100-doped PDMS. (B) Schematic of the silanization reaction between a methoxysilane molecule and an oxygen plasma-treated PDMS surface. In this work, a PEG-functional silane was used. (C) Water contact angle on PDMS modified with PEG (6–9)-silane and PDMS modified with PEG (21–24)-silane. (D) Water contact angle change after heat on plasma-oxidized pure PDMS, 0.5% TritonX100-doped PDMS (plasma-oxidized), and PDMS modified with PEG (6–9)-silane.

chip and adding PCR mix did not lead to additional cell loss. The results prove that this micro-well array has a great potential for rare cell detection due to its high rate of single cell loading and low cell loss data.

3.2. Effect of PEG-coated micro-well array

The hydrophobicity of the PDMS surface results in strong adsorption of proteins, which was the major obstacle for the highly sensitive detection of genes from single cells. The most common hydrophilic modification of PDMS is oxygen plasma treatment. Nevertheless, this hydrophilicity is only temporary as the PDMS surface will rapidly recover its hydrophobicity(Kim et al., 2000). Surfactants can be doped into pre-cured PDMS to modify its surface properties, yet this permits less nonspecific adsorption of protein. Based on a previous study (Fu et al., 2017), we chose 0.5% TritonX100-doped PDMS to fabricate the micro-well array. The contact angle of the surfactant-modified PDMS surface decreased gradually over time (Fig. 3A), showing strong hydrophilicity and stability up to 60 min. Conversely, the contact angle of pure PDMS remained above 100°. Herein, PCR on the TritonX100-doped PDMS micro-well array chip failed, likely due to TritonX100 not permitting tight bonding between the chip and glass. In addition, the volume of each unit in this micro-well array was seven-fold less than that used in the previous chip(Fu et al., 2017), while the improvement of PCR efficiency by surfactant modification was not sufficient. Therefore, the TritonX100 doping method cannot solve the low efficiency of PCR on this micro-well chip.

Surface modification methods based on covalent binding strive to combine multiple strategies (Zhang et al., 2011). Herein, oxygen plasma treatment produced a –OH layer on the surface of pure PDMS, which was then reacted with PEG-silane, resulting in a hydrophilic layer (Fig. 3B). Reactive sites on the PDMS surface after plasma treatment are transient, and the length of the PEG chain was a key parameter in creating a stable and valid surface modification(Kovach et al., 2014). To explore the modification effect of different carbon chain lengths in PEG silane, we compared the dynamic contact angle between a PDMS chip modified with PEG (6–9)-silane and that with PEG (21–24)-silane (Fig. 3C). The results showed that the PEG (6–9)-silane-coated PDMS chip was highly hydrophilic and remained stable over time. While the contact angle of the PEG (21–24)-silane-modified PDMS chip was in the range of 70–85° and changed little over time. Therefore, PEG (6–9)-silane modification was used to process the PDMS chip in subsequent experiments.

To achieve highly efficient PCR on a PDMS chip at a micro-volume, the PDMS surface should maintain its hydrophilicity in the long term

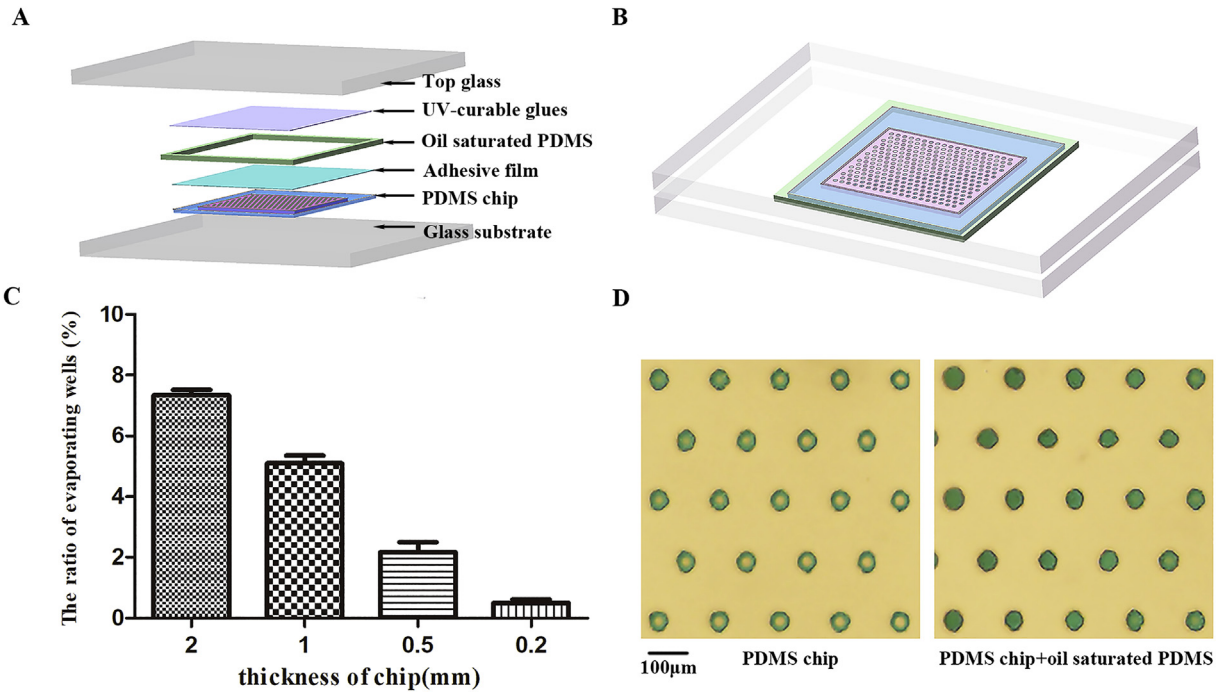

Fig. 4. Chip sealing and optimization of chip thickness. (A) Schematic of the layered chip structure. (B) Schematic of sealed chip. In the optimization experiments, a blue dye solution was used instead of samples in order to observe easily. (C) Comparison of water loss in the middle PDMS layer of different thickness during thermocycling. (D) Comparison of evaporation on PDMS chip and PDMS chip sealed with oil-saturated PDMS. (For interpretation of the references to colour in this figure legend, the reader is referred to the Web version of this article.)

and during temperature circulation. Therefore, we examined the wettability changes of the modified PDMS chips before and after the PCR process (Fig. 3D). The PEG-coated PDMS displayed the least change in contact angle following the high temperature treatment, and retained a strong hydrophilicity, while the contact angle of pure PDMS and 0.5% TritonX100-doped PDMS changed significantly and became weakly hydrophobic. These results indicated that the PEG grafting method can maintain hydrophilicity and is less affected by high temperatures, thus providing a good environment for on-chip PCR.

To verify the feasibility of on-chip PCR, we detected DNA of the same concentration (10^4 copies/μL) in micro-well arrays fabricated by unmodified PDMS and PEG-coated PDMS, respectively. There were no fluorescence signals detected in the unmodified PDMS chip due to inhibition. In contrast, the signals in the PEG-coated PDMS chip had a high signal-to-noise ratio because of the reduced inhibition for PCR (Fig. S4). Therefore, no complicated protocols are needed, only oxygen plasma treatment and incubation for 1 h to allow the PDMS chip strong and stable hydrophilicity. Thus, the PEG (6–9)-silane grafting method was used for PDMS modification.

3.3. Selective film for chip sealing and optimization of chip thickness

The micro-wells on the chip were open and independent structures without inlets and micro-channels. After sampling, the chip required sealing to form closed PCR reaction units. The chip construction is shown in Fig. 4A. An adhesive film was attached on the top of the chip, and then UV-curable glues were used to coat above the film and around the edge of the chip, followed by a glass being placed on the top to form a 'sandwich' structure (Fig. 4B). Compared with PDMS doped with mineral oil, the UV-curable glue-coated sandwich chip was tighter, without the appearance of dry micro-wells after PCR (Fig. S5). In addition to ensuring a firm adhesion between the glass and the film, selecting a suitable sealing film is also of importance for the PDMS chip package. We compared the chip sealing conditions with three different adhesive-encapsulating films after PCR. The parameters and sealing effect of the three films are listed in Table S1. The polypropylene double-side adhesive film had moderate thickness and strong adhesion, and allowed close and firm bonding to the PDMS chip. Compared to the previously reported sealing method (Gong et al., 2010; Wang et al., 2016), the adhesive film was able to separate every micro-well and allow extra solutions be removed completely through centrifugation. Therefore, the polypropylene double-sided adhesive film was selected to seal the micro-well array herein.

The porosity of PDMS will lead to water diffusion and rapid evaporation during the thermal cycling process(Christiansen and Rajasekaran, 2006), presenting a serious problem for micro-wells with a high surface-to-volume ratio. To reduce water diffusion, the top and bottom glasses in the packaged chip provided two protection layers for the micro-wells. However, the side areas of the PDMS chip were exposed to air, resulting in water loss. Water vapor diffusion and diffusion area are directly proportional to one another, according to on Fick's laws of diffusion(Fu et al., 2017).Therefore, the thicker the PDMS chip, the larger the diffusion area. Here, a blue dye solution was used as sample to facilitate visualization. The degree of evaporation of micro-wells after PCR was compared between four PDMS chips of varying thickness (Fig. 4C), showing that water loss decreased with reducing PDMS thickness. Additionally, applying uncured mineral oil-doped PDMS around the packaged chip led to further prevention of water vapor diffusion (Fig. 4D).

3.4. Proof-of-principle: detection of nuclear acids extracted from lung cancer cells

To verify the PCR efficiency of the developed micro-well array, we detected EGFR gene exon 21 in a series of H1975 gDNA samples ranging from 10^1 to 10^5 copies/μL using the micro-well array. The process of detecting nuclear acids with this micro-well array is shown in Fig. 5A and B. It is equivalent to partitioning the DNA template into 26,208 independent micro-wells. The concentration of nuclear acids detected with the micro-well array can be calculated according the Poisson

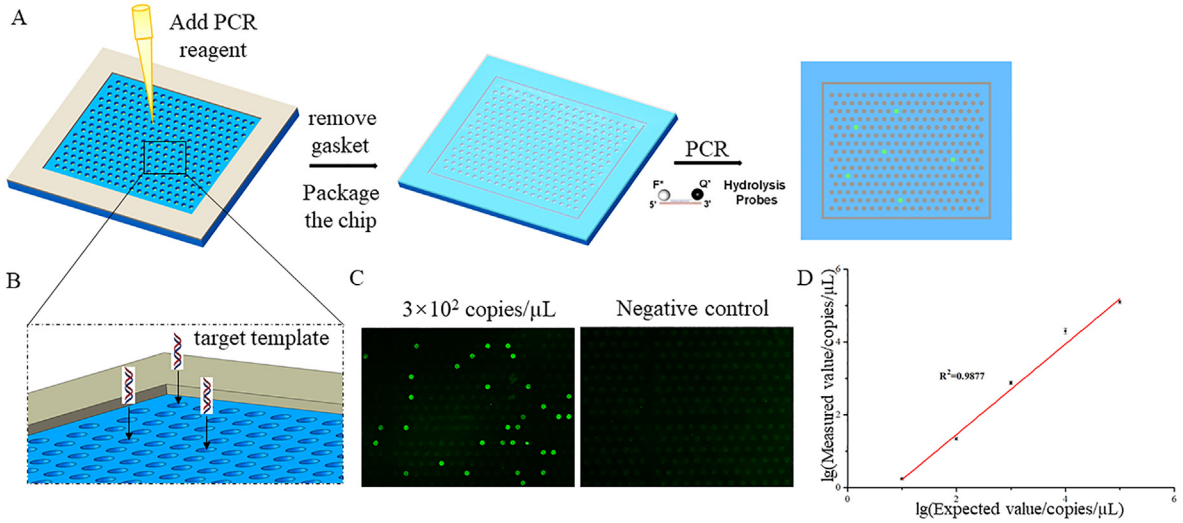

Fig. 5. The design and operation of the micro-well array device for digital PCR. (A) Process for detection of nuclear acids with the micro-well chip. Firstly, the PCR mix with the target template was directly loaded onto the micro-well array device. Secondly, the chip was sealed with polypropylene double-sided adhesive film and glass. The device was then placed into a thermocycler for PCR amplification. Multigene expression via up to two off-the-shelf hydrolysis probes with whole chip signals were imaged by fluorescence microscopy. (B) Template loading onto the chip. (C) Image of 3×10^2 copies/μL of DNA and no DNA detected by this chip. Scale bars 100 μm. (D) The measured value (copies/μL) in the micro-well array assay against its expected values. The graph is represented in a log-log format. Error bars depict 95% confidence intervals.

distribution as other chamber-based digital PCR chips (Fu et al., 2017; Wu et al., 2017). The image results of the 3×10^2 copy/μL DNA template and negative control were shown in Fig. 5C. Based on the amounts of positive and negative units, a standard curve for nuclear acids detected was draw, with the results showing a good match with the expected concentrations ($R^2 = 0.9877$; Fig. 5D). The above measurements indicate that the chip can perform highly efficient PCR amplification in a small-volume ($Vd = 25^2\pi \times 20\,\mu m^3 = 98\,pL$) PCR reaction system. The high efficiency of PCR on the chip provides strong support for the highly sensitive detection of low-copy genes from single cells.

3.5. Cell lysis in situ

The key to single-cell genetic testing on chip is how to release the target gene from single cells in situ without affecting subsequent PCR. Commonly used lysis methods for cells include enzymatic catalysis, heating(White et al., 2013) and chemical lysis(Han et al., 2014). To verify the effect of single cell lysis on the micro-well array, we loaded H1975 cells in chip and lysed the cells by proteinase K and heating, respectively. EGFR exon 21 gene of single cells was subsequently detected in situ. We didn't observe any positive signals in the sample lysed by proteinase K. While positive signals were detected in the sample treated by heat lysis (Fig. S6). The nucleic acids released from cells after proteinase K treatment were lost during adding PCR mix, leading to no positive signals. The process of lysing cells by heating was first heated at 75 °C for 7 min and then cooled at 4 °C. After this process, blurred cell contours were also observed, and nucleic acids in the cells were not released into the solution. Therefore, there was no nucleic acid loss during adding the PCR master mix. During the process of 50 °C for 30 min, the nucleic acids were released and amplified in the subsequent PCR. The results further demonstrated heat lysis in situ was compatible with PCR on chip. And the heating temperature for cell lysis was optimized (shown in Fig. S7). Under 65 °C, proteins in the cells were not completely denatured, resulting in incomplete cell lysis and no release of nucleic acid. Above 85 °C, no fluorescence signals were detected. 75 °C is selected as the optimum temperature to process cells in subsequent experiment.

3.6. Duplex EGFR point mutation detection in single tumor cells with micro-well array

Detection of EGFR mutations for lung cancer is of great importance to provide guidance for targeted therapy decisions (Lee et al., 2016; Mohar et al., 2016). Approximately 15% of lung adenocarcinoma patients worldwide have EGFR mutations, which is twice as high in the Asian population (Kobayashi et al., 2005). While resistance inevitably occurs in lung patients with EGFR-driver mutations during treatment. Currently, the efficacy can only be monitored by extraneous methods, such as imaging or clinical symptoms. Recent reports suggest that CTCs may be a new biomarker for monitoring treatment of lung cancer (Gao et al., 2018; Oulhen et al., 2018; Sundaresan et al., 2016).

Firstly, we tested EGFR exon gene 20 and 21 in the extracts from 10^6 normal leukocytes, A549, and H1975 cells by real-time quantitative PCR and the Sanger sequence, respectively. EGFR exon gene 20 and 21 were wild type in A549 cells and normal leukocytes (Fig. S8A). While EGFR T790M and L858R point mutations occurred in H1975 cells (Fig. S8B). Then we used micro-well arrays to detect EGFR exon gene at the single-cell level in normal leukocytes, A549, and H1975 cells. The three cell types were loaded in a chip and stained with immunofluorescence antibodies in-situ. Leukocytes were bound to anti-CD45 antibodies conjugated to phycoerythrin and labeled orange. Anti-CK antibodies conjugated to isothiocyanate were specifically bound to A549 and H1975 cells, which were marked as green. Chips were observed with a fluorescence microscope after immunofluorescence staining. The EGFR exon gene 20 and 21 in single cells were subsequently measured on the micro-well array. Normal leukocytes and A549 cells exhibited negative EGFR L858R and T790M mutation signals. H1975 cells revealed positive signals for either EGFR L858R or T790M mutation (Fig. 6A). Average of EGFR exon gene 20 and 21 expression was similar among white blood cells, A549 and H1975 cells (Fig. S9). Micro-well confirmed differential EGFR L858R and T790M expression between normal leukocytes, A549 and H1975 cells, with individual leukocytes and A549 cells only expressing wild-type EGFR($P < 0.01$)(Fig. 6B). The individual-cell level of EGFR expression for leukocytes and A549 cells was consistent with bulk cells analysis. The majority of H1975 cells occurred EGFR L858R or T790M mutation. Duplex detection of EGFR L858R and EGFR T790M in single H1975 cells indicated that not all H1975 cells had double-point mutations, and some cells had either

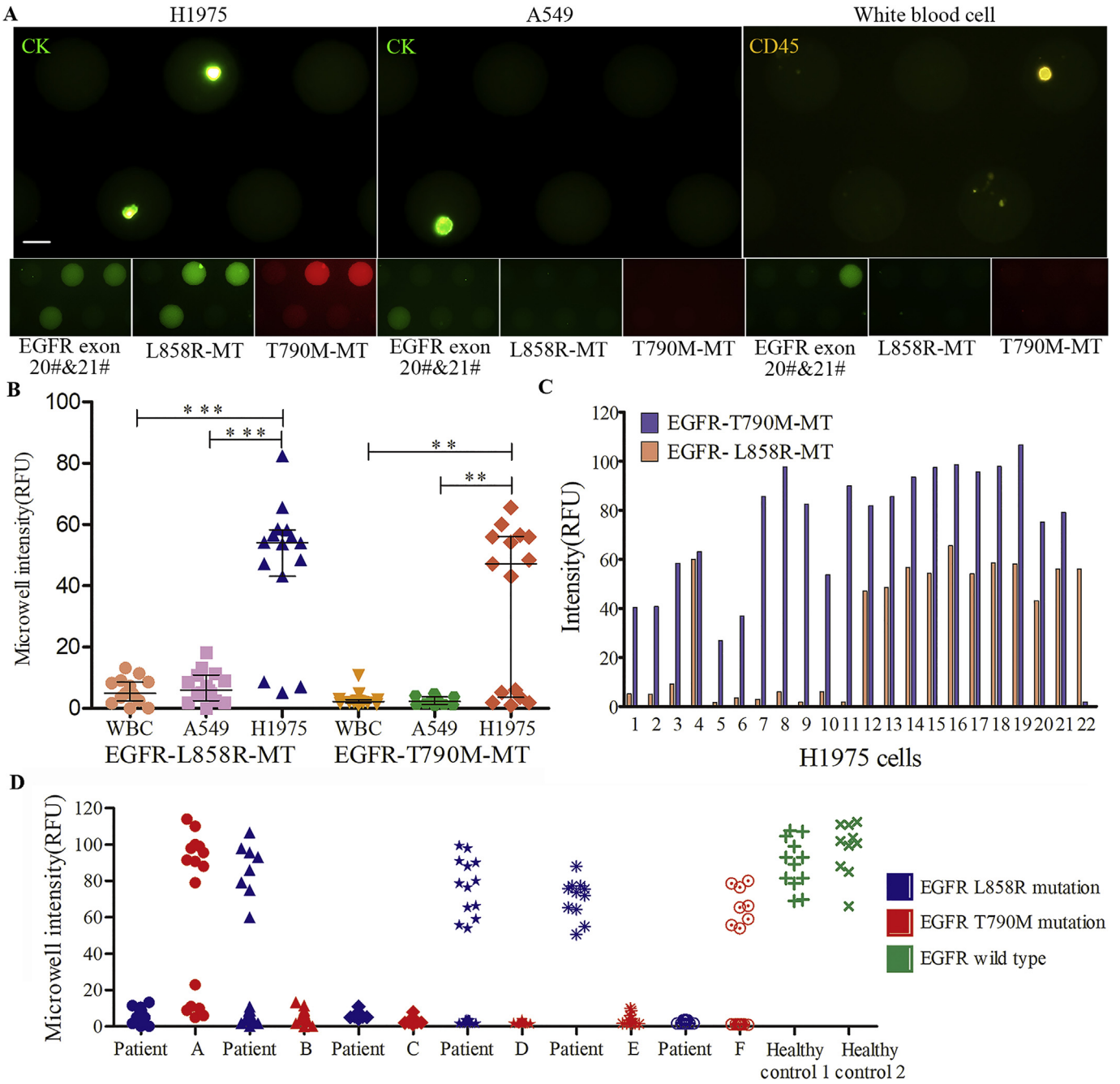

Fig. 6. Validation of our integrated micro-well array-based system with lung cancer cell lines and clinical samples. (A) Images of single-cell analysis from H1975, A549, and white blood cells. H1975, A549, and white blood cells were stained with immunofluorescence antibodies (CD45-PE and CK-FITC) and then they each underwent single-cell analysis on the micro-well using both EGFR exon gene 20 and 21 probes in the HEX channel (shown in green), EGFR-L858R in the FAM channel (shown in green), and EGFR-T790M in the ROX channel (shown in red). A549 and white blood cells exhibited fluorescence only in the HEX channel, indicating the presence of wild-type EGFR. In contrast, some H1975 cells exhibited fluorescence in both FAM and ROX channels, indicating the presence of EGFR-L858R and EGFR-T790M. Scale bars 20 μm. (B) Single-cell analysis using micro-well on H1975, A549, and white blood cells by RT-PCR expression analysis of EGFR L858R and T790M mutant. Micro-wells showed a clear differentiation between H1975 and A549 cells based on EGFR L858R and T790M mutant expression, with high statistical significance (n = 15, ***P < 0.0001, **P < 0.01), as well as H1975 and white blood cells. (C) Expression levels of EGFR L858R and T790M mutations in a single H1975 cell. (D) Expression levels of EGFR exon gene in CTCs from six advanced lung patients and white blood cells from two healthy controls. Each CTC was identified by immunofluorescence staining (CD45-/CK + cells). (For interpretation of the references to colour in this figure legend, the reader is referred to the Web version of this article.)

EGFR L858R mutation or EGFR T790M mutation (Fig. 6C).While in the bulk cell genetic testing experiment, the point mutation in single H1975 cells was unclear. In addition, in comparing genetic detection with protein expression in the same micro-well, some CK-negative cells had detectable EGFR L858R and T790M mutation (H1975 cell in Fig. 6A), indicating that this genetic analysis method can provide complementary information for conventional CTC identification. These results demonstrate that the micro-well array can undergo duplex gene detection for single tumor cells in high throughput and be integrated with the traditional fluorescent immunostaining to provide molecular characteristics for CTC detection.

To evaluate the detection performance of this micro-well array for

lung CTCs, blood samples from patients with lung cancer and healthy person were enriched for CTCs with the anti-CD45 antibody-modified magnetic beads. The cell left after the process, including CTCs, were fluorescently stained and genetically analyzed using our designed device. EGFR L858R and T790M mutations were simultaneously detected in enriched cells from six patients at lung adenocarcinoma stage IV with known EGFR types and two healthy persons. Each CTCs (CD45-/CK +/DAPI + cells) were identified based on immunofluorescence assay. Heterogeneous expression of EGFR exon 20 and 21 mutational genes were observed in CTCs from five patients (Fig. 6D). No mutational genes were detected in patient C and two healthy controls. The single-cell mutational gene types of CTCs from these six patients were consistent with the genetic type of their pathological cells detected in clinical tests (Table S2). In addition, we found that both EGFR L858R and T790M were detected in some CK-/CD45-cells from lung cancer patient A and B, which were not recognized as CTCs by common identification standard (Fig. S10). Although different levels and types of EGFR expression in those CTCs were detected, further work focusing on these patients' clinical outcomes is necessary for accurate diagnosis and treatment.

Compared to single-cell genetic mutation detection methods that rely on the ICC recognition of CTCs and manually retrieving single cells (Chen et al., 2013; Zhang et al., 2015), our method has the advantage of high throughput and low cell loss. In addition, the low cost (with reagent costs of ~30 US dollars per test) and simple-performance are beneficial to clinical application to guide targeted therapy strategies. We envision that the micro-well array will be used as a practical tool to rapidly screen important mutations on CTCs discovered by whole-genome sequencing. But this method reported here still has some limitations. We have only demonstrated duplex mutational EGFR genes in single lung CTCs. Further assay development with multiple detection for EGFR exon genes 19, 18, and 21 will be attempted with this method.

4. Conclusions

In this study, we have developed a micro-well array-based detection platform for high-throughput and simultaneously multiplex genetic analysis at the single-cell level. This chip can achieve a high loading rate (over 90%) of cells through centrifugation, eliminating the requirement for external pumping and valves. On the one hand, this micro-well array with a small PCR reaction unit (98 pL) revealed a sensitive quantification capability, providing strong support for low copy nucleic acid detection for CTCs. On the other hand, we successfully integrated cell capture, lysis, PCR amplification, and signal readout on the PDMS made micro-well array, allowing single-cell gene detection simple and low-cost. Heterogeneous mutations (EGFR-L858R mutation or EGFR-T790M mutation) were detected in H1975 cells and CTCs from lung cancer patient samples, which further validated the significance of CTC single-cell level gene detection. But how CTC genetic heterogeneity relates to patient clinical symptoms and outcome is an important and valuable research, requiring further inquiry in the future. Even though, this micro-well array platform has been shown to be a convenient and accurate tool for CTC genetic analysis at the single-cell level and is expected to facilitate lung cancer diagnosis and therapy selection.

CRediT authorship contribution statement

Wanlei Gao: Conceptualization, Methodology, Data curation, Writing - original draft. **Xiaofen Zhang:** Methodology, Validation, Data curation. **Haojun Yuan:** Conceptualization, Methodology, Data curation, Writing - original draft. **Yanmin Wang:** Visualization, Investigation. **Hongbo Zhou:** Supervision. **Han Jin:** Data curation, Software, Validation. **Chunping Jia:** Writing - review & editing, Supervision. **Qinghui Jin:** Project administration, Resources. **Hui Cong:** Supervision, Resources. **Jianlong Zhao:** Project administration, Resources.

Acknowledgments

This work was financially supported by the grants from the National Key Research and Development Program of China (No. 2017YFA0205303, 2017ZX10302201-005-006), the National Natural Science Foundation of China (No. 61871243, 61671284, and 61801465) ,the Program of Science and Technology Commission of Shanghai Municipality (No.17JC1401001), Research project of scientific research equipment of CAS (No. YJKYYQ20170043), STS program (No. KFJ-STS-ZDTP-061), the science and technology support plan of the Shanghai Science and Technology Committee (No. 17441904300), Zhejiang provincial natural science foundation (No.LQ19F010004),and China Postdoctoral Science Foundation(No.2018M642384).And this study was also sponsored by K.C.Wong Magna Fund in Ningbo University.

Appendix A. Supplementary data

Supplementary data to this article can be found online at https://doi.org/10.1016/j.bios.2019.111326.

References

Alberter, B., Klein, C.A., Polzer, B., 2016. Single-cell analysis of CTCs with diagnostic precision: opportunities and challenges for personalized medicine. Expert Rev. Mol. Diagn 16 (1), 25–38.
Chen, C.L., Mahalingam, D., Osmulski, P., Jadhav, R.R., Wang, C.M., Leach, R.J., Chang, T.C., Weitman, S.D., Kumar, A.P., Sun, L., Gaczynska, M.E., Thompson, I.M., Huang, T.H., 2013. Single-cell analysis of circulating tumor cells identifies cumulative expression patterns of EMT-related genes in metastatic prostate cancer. Prostate 73 (8), 813–826.
Christiansen, J.J., Rajasekaran, A.K., 2006. Reassessing epithelial to mesenchymal transition as a prerequisite for carcinoma invasion and metastasis. Cancer Res. 66 (17), 8319–8326.
Dancey, J.E., Bedard, P.L., Onetto, N., Hudson, T.J., 2012. The genetic basis for cancer treatment decisions. Cell 148 (3), 409–420.
Devriese, L.A., Bosma, A.J., van de Heuvel, M.M., Heemsbergen, W., Voest, E.E., Schellens, J.H.M., 2012. Circulating tumor cell detection in advanced non-small cell lung cancer patients by multi-marker QPCR analysis. Lung Cancer 75 (2), 242–247.
Dimov, I.K., Lu, R., Lee, E.P., Seita, J., Sahoo, D., Park, S.M., Weissman, I.L., Lee, L.P., 2014. Discriminating cellular heterogeneity using microwell-based RNA cytometry. Nat. Commun. 5, 3451.
Fu, Y.Y., Zhou, H.B., Jia, C.P., Jing, F.X., Jin, Q.H., Zhao, J.L., Li, G., 2017. A microfluidic chip based on surfactant-doped polydimethylsiloxane (PDMS) in a sandwich configuration for low-cost and robust digital PCR. Sensor. Actuator. B Chem. 245, 414–422.
Gao, W.L., Huang, T., Yuan, H.J., Yang, J., Jin, Q.H., Jia, C.P., Mao, G.X., Zhao, J.L., 2018. Highly sensitive detection and mutational analysis of lung cancer circulating tumor cells using integrated combined immunomagnetic beads with a droplet digital PCR chip. Talanta 185, 229–236.
Gong, Y., Ogunniyi, A.O., Love, J.C., 2010. Massively parallel detection of gene expression in single cells using subnanolitre wells. Lab Chip 10 (18), 2334–2337.
Haber, D.A., Velculescu, V.E., 2014. Blood-based analyses of cancer: circulating tumor cells and circulating tumor DNA. Cancer Discov. 4 (6), 650–661.
Haider, M., Ji, B., Haselgrubler, T., Sonnleitner, A., Aberger, F., Hesse, J., 2016. A microfluidic multiwell chip for enzyme-free detection of mRNA from few cells. Biosens. Bioelectron. 86, 20–26.
Han, L., Zi, X., Garmire, L.X., Wu, Y., Weissman, S.M., Pan, X., Fan, R., 2014. Co-detection and sequencing of genes and transcripts from the same single cells facilitated by a microfluidics platform. Sci. Rep. 4, 6485.
Katanoda, K., Saito, E., Hori, M., 2018. Cancer statistics - past trends and future perspectives. Cancer Sci. 109 773-773.
Kim, J., Chaudhury, M.K., Owen, M.J., 2000. Hydrophobic recovery of polydimethylsiloxane elastomer exposed to partial electrical discharge. J. Colloid Interface Sci. 226 (2), 231–236.
Kobayashi, S., Boggon, T.J., Dayaram, T., Janne, P.A., Kocher, O., Meyerson, M., Johnson, B.E., Eck, M.J., Tenen, D.G., Halmos, B., 2005. EGFR mutation and resistance of non-small-cell lung cancer to gefitinib. N. Engl. J. Med. 352 (8), 786–792.
Kovach, K.M., Capadona, J.R., Gupta, A.S., Potkay, J.A., 2014. The effects of PEG-based surface modification of PDMS microchannels on long-term hemocompatibility. J. Biomed. Mater. Res. A 102 (12), 4195–4205.
Krebs, M.G., Metcalf, R.L., Carter, L., Brady, G., Blackhall, F.H., Dive, C., 2014. Molecular analysis of circulating tumour cells-biology and biomarkers. Nat. Rev. Clin. Oncol. 11 (3), 129–144.
Lee, S.E., Lee, S.Y., Park, H.K., Oh, S.Y., Kim, H.J., Lee, K.Y., Kim, W.S., 2016. Detection of EGFR and KRAS mutation by pyrosequencing analysis in cytologic samples of non-small cell lung cancer. J. Korean Med. Sci. 31 (8), 1224–+.

Lin, M., Chen, J.F., Lu, Y.T., Zhang, Y., Song, J., Hou, S., Ke, Z., Tseng, H.R., 2014. Nanostructure embedded microchips for detection, isolation, and characterization of circulating tumor cells. Acc. Chem. Res. 47 (10), 2941–2950.

Lin, Y.T., Yu, C.J., Yang, J.C.H., Shih, J.Y., 2016. Anaplastic lymphoma kinase (ALK) kinase domain mutation following ALK inhibitor(s) failure in advanced ALK positive non-small-cell lung cancer: analysis and literature review. Clin. Lung Cancer 17 (5), E77–E94.

Lu, X.Y., Yu, L., Zhang, Z., Ren, X.M., Smaill, J.B., Ding, K., 2018. Targeting EGFR(L858R/T790M) and EGFR(L858R/T790M/C797S) resistance mutations in NSCLC: current developments in medicinal chemistry. Med. Res. Rev. 38 (5), 1550–1581.

Maheswaran, S., Sequist, L.V., Nagrath, S., Ulkus, L., Brannigan, B., Collura, C.V., Inserra, E., Diederichs, S., Iafrate, A.J., Bell, D.W., Digumarthy, S., Muzikansky, A., Irimia, D., Settleman, J., Tompkins, R.G., Lynch, T.J., Toner, M., Haber, D.A., 2008. Detection of mutations in EGFR in circulating lung-cancer cells. N. Engl. J. Med. 359 (4), 366–377.

Mohar, B., Jezek, S.S., Molek, K.R., Stemberger, C., Kurpis, M., Kupanovac, Z., Samarzija, M., Jonjic, N., Grahovac, B., 2016. Detection of an EGFR mutation in cytological specimens of lung adenocarcinoma. Cytopathology 27 (6), 444–451.

Myung, J.H., Hong, S., 2015. Microfluidic devices to enrich and isolate circulating tumor cells. Lab Chip 15 (24), 4500–4511.

Novak, R., Zeng, Y., Shuga, J., Venugopalan, G., Fletcher, D.A., Smith, M.T., Mathies, R.A., 2011. Single-cell multiplex gene detection and sequencing with microfluidically generated agarose emulsions. Angew. Chem. Int. Ed. 50 (2), 390–395.

O'Flaherty, J.D., Gray, S., Richard, D., Fennell, D., O'Leary, J.J., Blackhall, F.H., O'Byrne, K.J., 2012. Circulating tumour cells, their role in metastasis and their clinical utility in lung cancer. Lung Cancer 76 (1), 19–25.

Oulhen, M., Aberlenc, A., Pailler, E., Faugeroux, V., Mezquita, L., Honore, A., Remon, J., Lacroix, L., Lecluse, Y., Manaresi, N., Ngocamus, M., Nicotra, C., Planchard, D., Soria, J.C., Besse, B., Farace, F., 2018. Detection of activating and resistance mutations in single CTCs from EGFR-mutant non-small cell lung cancer patients treated by EGFR inhibitors. Clin. Exp. Metastasis 35 (3) 204-204.

Rothschild, S.I., 2016. New treatment options for ALK plus advanced non-small-cell lung cancer: critical appraisal of ceritinib. Therapeut. Clin. Risk Manag. 12.

Shen, S.F., Ma, C., Zhao, L., Wang, Y.L., Wang, J.C., Xu, J., Li, T.B., Pang, L., Wang, J.Y., 2014. High-throughput rare cell separation from blood samples using steric hindrance and inertial microfluidics. Lab Chip 14 (14), 2525–2538.

Sundaresan, T.K., Sequist, L.V., Heymach, J.V., Riely, G.J., Janne, P.A., Koch, W.H., Sullivan, J.P., Fox, D.B., Maher, R., Muzikansky, A., Webb, A., Tran, H.T., Giri, U., Fleisher, M., Yu, H.A., Wei, W., Johnson, B.E., Barber, T.A., Walsh, J.R., Engelman, J.A., Stott, S.L., Kapur, R., Maheswaran, S., Toner, M., Haber, D.A., 2016. Detection of T790M, the acquired resistance EGFR mutation, by tumor biopsy versus non-invasive blood-based analyses. Clin. Cancer Res. 22 (5), 1103–1110.

Tang, M., Wen, C.Y., Wu, L.L., Hong, S.L., Hu, J., Xu, C.M., Pang, D.W., Zhang, Z.L., 2016. A chip assisted immunomagnetic separation system for the efficient capture and in situ identification of circulating tumor cells. Lab Chip 16 (7), 1214–1223.

Tartarone, A., Rossi, E., Lerose, R., Mambella, G., Calderone, G., Zamarchi, R., Aieta, M., 2017. Possible applications of circulating tumor cells in patients with non small cell lung cancer. Lung Cancer 107, 59–64.

Wang, Y., Southard, K.M., Zeng, Y., 2016. Digital PCR using micropatterned superporous absorbent array chips. Analyst 141 (12), 3821–3831.

White, A.K., Heyries, K.A., Doolin, C., Vaninsberghe, M., Hansen, C.L., 2013. High-throughput microfluidic single-cell digital polymerase chain reaction. Anal. Chem. 85 (15), 7182–7190.

Wu, L.J., Pan, Y.D., Pei, X.Y., Chen, H., Nguyen, S., Kashyap, A., Liu, J., Wu, J., 2012. Capturing circulating tumor cells of hepatocellular carcinoma. Cancer Lett. 326 (1), 17–22.

Wu, Z.H., Bai, Y.N., Cheng, Z.L., Liu, F.M., Wang, P., Yang, D.W., Li, G., Jin, Q.H., Mao, H.J., Zhao, J.L., 2017. Absolute quantification of DNA methylation using microfluidic chip-based digital PCR. Biosens. Bioelectron. 96, 339–344.

Yu, L., Ng, S.R., Xu, Y., Dong, H., Wang, Y.J., Li, C.M., 2013. Advances of lab-on-a-chip in isolation, detection and post-processing of circulating tumour cells. Lab Chip 13 (16), 3163–3182.

Zhang, Y., Tang, Y., Sun, S., Wang, Z., Wu, W., Zhao, X., Czajkowsky, D.M., Li, Y., Tian, J., Xu, L., Wei, W., Deng, Y., Shi, Q., 2015. Single-cell codetection of metabolic activity, intracellular functional proteins, and genetic mutations from rare circulating tumor cells. Anal. Chem. 87 (19), 9761–9768.

Zhang, Z.Y., Wang, J.C., Tu, Q., Nie, N., Sha, J., Liu, W.M., Liu, R., Zhang, Y.R., Wang, J.Y., 2011. Surface modification of PDMS by surface-initiated atom transfer radical polymerization of water-soluble dendronized PEG methacrylate. Colloids Surf., B 88 (1), 85–92.

Zou, B., Lee, V.H.F., Chen, L.J., Ma, L.C., Wang, D.D., Yan, H., 2017. Deciphering mechanisms of acquired T790M mutation after EGFR inhibitors for NSCLC by computational simulations. Sci Rep-Uk 7.